Complete Control of Population Transfer between Clusters of Degenerate States

Ioannis Thanopulos, Petr Král, and Moshe Shapiro

Department of Chemical Physics, The Weizmann Institute of Science, Rehovot 76100, Israel
Departments of Chemistry and Physics, The University of British Columbia, Vancouver, Canada V6T1Z1

(Received 26 June 2003; published 18 March 2004)

We present an analytic solution to the "degenerate quantum control problem," which enables the transfer of any desired fraction of population between *arbitrary initial* and *final* pure wave packets, made up of *nearly degenerate* energy eigenstates. It consists of two two-photon adiabatic passage steps, in which the population of the initial wave packet is first transferred, via a number of nondegenerate intermediate states, to a single eigenstate and then returned to a different target superposition state. We demonstrate the approach by executing a stepwise isomerization of three Jahn-Teller states of the Al_3O molecule, where a proper optical coupling can easily be established.

DOI: 10.1103/PhysRevLett.92.113003 PACS numbers: 32.80.Qk, 33.15.Bh, 33.80.–b, 42.50.Hz

Coherent control techniques use multiply interfering quantum pathways [1] to *selectively* transfer population to desired target states. In a complementary way, adiabatic passage methods [2,3] enable the *complete* population transfer between quantum states. Recently, both techniques have been merged to achieve *both* selectivity and completeness. With this approach [4], we have been able to show how to purify a mixture of left-handed and right-handed chiral molecules by several pulses.

The universality of the adiabatic passage techniques was also greatly increased when they were applied in the addressing or readdressing of several final degenerate states [5–7]. An important extension of the (three-state) adiabatic passage [3] was to act on wave packets composed of many *nondegenerate* states [8]. We have thus solved the "nondegenerate quantum control" (NQC) problem, i.e., how to achieve a complete population transfer between an arbitrary initial $|\Psi_i\rangle = \sum_k c_{i,k}\, e^{-i\omega_k t}\,|k\rangle$ and a target $|\Psi_f\rangle = \sum_{k'} c_{f,k'} e^{-i\omega_{k'} t}\,|k'\rangle$ wave packet, formed of nondegenerate quantum states. This transfer is realized by a multipath two-photon process, proceeding via a single intermediate eigenstate, to which all the nondegenerate states are resonantly coupled.

In this work, we further pave the way leading to the complete control of quantum systems. We solve the "degenerate quantum control" (DQC) problem, i.e., how to transfer population between arbitrary pure wave packets, $|\Psi_i\rangle \approx e^{-i\omega_i t}\sum_k c_{i,k}|k\rangle$ and $|\Psi_f\rangle \approx e^{-i\omega_f t}\sum'_k c_{f,k'}|k'\rangle$, composed of *nearly degenerate* energy eigenstates, for which the nearest-neighbor separations are much smaller than the bandwidth of the laser pulses used. We can *separately* address all the nearly degenerate levels, $|k\rangle$ and $|k'\rangle$, by coupling each of them *differently* to all of the many nondegenerate eigenstates, $|j\rangle$ and $|j'\rangle$, that form intermediate states of the applied two-photon processes. By controlling the interference processes accompanying this simultaneous multilevel coupling, we can achieve the full generality of the DQC solution.

We solve DQC in two steps, illustrated in Fig. 1. In step 1 (upper panel), we use a pair of laser pulses to adiabatically transfer the population of the initial wave packet $|\Psi_i\rangle$ ($|1\rangle_{\rm loc}$), composed of the nearly degenerate

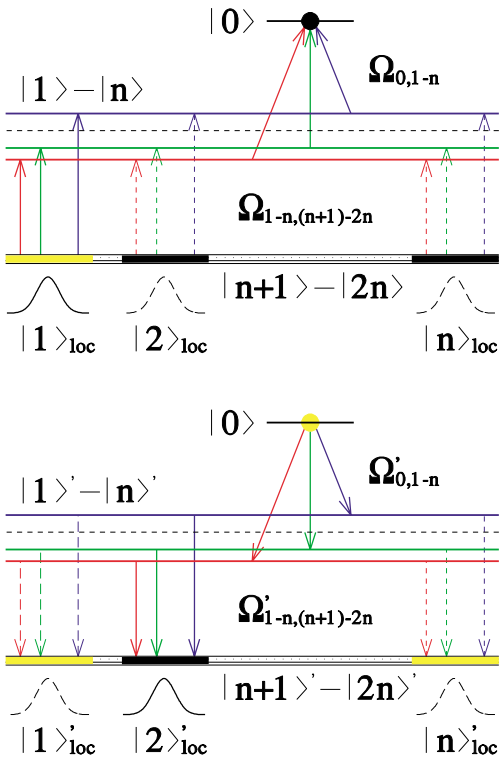

FIG. 1 (color online). The DQC scheme. (Upper panel) Step 1: population in a space-localized wave packet $|1\rangle_{\rm loc}$, composed of *n nearly degenerate* eigenstates, is transferred to a single state $|0\rangle$, by a two-photon adiabatic passage via *n nondegenerate* intermediate states. (Lower panel) Step 2: population transfer by a time reversed process with different Rabi frequencies from $|0\rangle$ to the target wave packet $|2\rangle'_{\rm loc}$, composed also of a set of nearly degenerate eigenstates.

energy eigenstates $|k\rangle$ $(k = n+1, \ldots, 2n)$, to a single ("parking") state $|0\rangle$, using the nondegenerate auxiliary states $|j\rangle$ $(j = 1, \ldots, n)$ as intermediates. The "dump" (D) pulse, linking the $|j\rangle$ states and the $|0\rangle$ state, characterized by Rabi frequencies $\Omega_{1,\ldots,n;0}$, is followed by a "pump" (P) pulse, linking the $|k\rangle$ states with *all* the $|j\rangle$ states, characterized by $\Omega_{n+1,\ldots,2n;1,\ldots,n}$. In step 2 (lower panel), the population in the parking state $|0\rangle$ is transferred, by time reversing the dump and pump pulses of step 1 and using different Rabi frequencies, to the target wave packet $|\Psi_f\rangle$ $(|2\rangle'_{\rm loc})$, composed of the same (or a different) set of nearly degenerate eigenstates $|k'\rangle$.

We now describe the pulses used in DQC. In the first step the total electric field is

$$\vec{\mathcal{E}}(t) = \mathcal{R}_e \sum_{j=1}^{n} \{\vec{\mathcal{E}}_{0,j}(t)\, e^{-i\omega_{0,j}t} + \vec{\mathcal{E}}_{j,i}(t)\, e^{-i\omega_{j,i}t}\}, \quad (1)$$

while in the second step $i \rightarrow f$ and the roles of the D and P pulses are *reversed*. The dump $\vec{\mathcal{E}}_{0,j}(t) = \hat{\boldsymbol{\epsilon}}_{0,j}\, \mathcal{E}_{0,j}(t)$ and pump $\vec{\mathcal{E}}_{j,i}(t) = \hat{\boldsymbol{\epsilon}}_{j,i}\, \mathcal{E}_{j,i}(t)$ field components are characterized by the polarization directions $\hat{\boldsymbol{\epsilon}}_{j,i}$ and the slowly varying amplitudes $\mathcal{E}_{0,j}(t)$ and $\mathcal{E}_{j,i}(t)$. The central frequencies of the field components are chosen to be near resonance with the system's transition frequencies, $\omega_{0,j} = \omega_0 - \omega_j$ and $\omega_{j,i} = \omega_j - \omega_i$. The complex Rabi frequencies, expressed in atomic units $(\hbar = 1)$, are $\Omega_{j,i}(t) \equiv \vec{\boldsymbol{\mu}}_{j,i} \cdot \vec{\mathcal{E}}_{j,i}(t)$, where $\vec{\boldsymbol{\mu}}_{j,i}$ are the transition-dipole matrix elements. They have *common* time envelopes, $\Omega_{j,i}(t) = \mathcal{O}_{j,i}\, f_{D(P)}(t)$, with f_D preceding f_P in both steps.

The system's wave function can be expanded in each step as $|\Psi\rangle = \sum_{i=0}^{2n} c_i(t) e^{-i\omega_i t}|i\rangle$, where the column vector $\mathbf{c}(t) = (c_0, c_1, \ldots, c_n, c_{n+1}, \ldots, c_{2n})$ of coefficients is obtained by solving the matrix Schrödinger equation, $\dot{\mathbf{c}}(t) = -i\mathsf{H}(t) \cdot \mathbf{c}(t)$. Here, $\mathsf{H}(t)$ denotes the effective Hamiltonian in the rotating waves approximation,

$$\mathsf{H}(t) = \begin{pmatrix} 0 & \Omega_0 & 0 \\ \Omega_0^\dagger & 0 & \mathbf{H}_F \\ 0 & \mathbf{H}_F^\dagger & 0 \end{pmatrix}, \qquad \mathbf{H}_F = \begin{pmatrix} \Omega_1 \\ \cdots \\ \Omega_n \end{pmatrix}, \quad (2)$$

and

$$\Omega_0 = (\Omega_{0,1}, \ldots, \Omega_{0,n}), \qquad \Omega_j = (\Omega_{j,n+1}, \ldots, \Omega_{j,2n}), \quad j = 1, \ldots, n, \quad (3)$$

with $\dagger$ denoting the adjoint operation. The Ω_{0-n} vectors of Rabi frequencies are different in the two steps because they control the population transfer between different wave packets.

We show that the two DQC steps can address or readdress arbitrary wave packets *only if* the Rabi vectors $\{\Omega_1, \ldots, \Omega_n\}$, which couple the $(k = n+1, \ldots, 2n)$ nearly degenerate levels to the $(j = 1, \ldots, n)$ nondegenerate levels, are *linearly independent*. In this case, $\mathcal{D} \equiv \det(\mathbf{H}_F) \neq 0$ and the Hamiltonian $\mathsf{H}(t)$ has just *one* zero eigenvalue, with the corresponding ("null" or "dark") eigenvector being given as $(1, \mathbf{0}, \mathbf{x})$, $\mathbf{0}$ denotes an n-dimensional zero vector, and $\mathbf{x}$ is an n-dimensional vector given as $\mathbf{x} = -\mathbf{H}_F^{-1}\Omega_0^\dagger$. Direct operation of $\mathsf{H}(t)$ on $(1, \mathbf{0}, \mathbf{x})$ confirms that this is the null state.

Then, if the Ω_0 vector of Eq. (3) is proportional to the kth column of the Hermitian $\mathbf{H}_F = \mathbf{H}_F^\dagger$ matrix, $\Omega_0^\dagger \propto \Omega_k^\dagger$ $(k = 1, \ldots, n)$, the $(1, \mathbf{0}, \mathbf{x})$ vector correlates at the end of step 1 (start of step 2) with the $|0\rangle$ state and at the start of step 1 (end of step 2) with the $|n+k\rangle$ nearly degenerate state. The linearity of the above equations guarantees that with the choice $\Omega_0^\dagger \propto \sum_{k=1}^{n} a_k \Omega_k^\dagger$ the null state is correlated at the start of step 1 (end of step 2) with the $\sum_{k=1}^{n} a_k |n+k\rangle$ superposition state. Thus, *complete control* over the population transfer between arbitrary wave packets, composed of nearly degenerate states, can be achieved. The efficiency of the two DQC steps is *not* lowered by the mutual *nonorthogonality* of the linearly independent vectors $\Omega_j^\dagger$ $(j = 1, \ldots, n)$. This is because the nonorthogonality is corrected for in the null vector, where $\Omega_0^\dagger (\propto \sum_{k=1}^{n} a_k \Omega_k^\dagger)$ gets multiplied by the $\mathbf{H}_F^{-1}$ matrix, which, according to Eq. (2), is the inverse of the $\Omega_k^\dagger$ $(k = 1, \ldots, n)$ matrix.

In addition to controlling arbitrary wave packets, we can choose, in both DQC and NQC [8] schemes, the *fraction* of population transferred. Thus, starting from an arbitrary initial $|\Psi_i\rangle = \sum_{k=n+1}^{2n} c_{i,k}|k\rangle$ wave packet and using $\Omega_0^\dagger = \sum_{k=1}^{n} a_k \Omega_k^\dagger$, where $a_k \neq c_{i,k}$, the amount of population transferred is given by the square of the scalar product, $|\mathbf{a} \cdot \mathbf{c}^{(i)}|^2$, of the $\mathbf{c}^{(i)} = (c_{i,n+1}, \ldots, c_{i,2n})$ and the $\mathbf{a} = (a_1, \ldots, a_n)$ vectors. In contrast to NQC, the second step of DQC can be executed effectively only if all the nearly degenerate final $|k\rangle$ states are initially empty. If these are populated at the start, $|\Psi_f\rangle = \sum_{k=n+1}^{2n} c_k^f |k\rangle$ (all $c_k^f \neq 0$), the vector amplitude $\mathbf{c}^{(f)}$ *cannot* be orthogonal to all the n linearly independent vectors Ω_l, which make up the dump pulse, and they are thus depopulated from the start.

Let us test the DQC solution on molecular systems with *several* quasistable (symmetry-related) configurations of equal energies. Chiral molecules, for example, possess two such configurations, the so-called enantiomers [4], while more configurations can be found in Jahn-Teller molecules [9]. As a particular example, we consider the Al_3O molecule, which possesses three local energy minima [10]. As shown in Fig. 2, they are characterized by C_{2v} planar T-shaped geometries, separated by three planar saddle points with C_{2v} Y-shaped configurations [10]. In order to achieve the desired transfer (pseudorotation) between the three T configurations, we hinder the overall rotation by (loosely) binding the molecule to a larger system, such as a solid surface or the inside of a large (inert) molecular "pocket" [11]. By doing so, we also *orient* the Al_3O molecule such that the out-of-plane motion of the O atom relative to the Al_3 triangle coincides with the z direction.

The three quasistable T configurations result in a set of triplet in-plane vibrational states. For energies well below the isomerization barrier, the eigenstates in each triplet

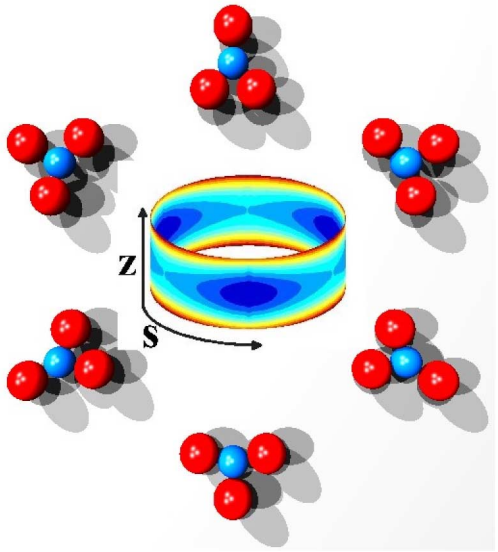

FIG. 2 (color online). The three Jahn-Teller minimum configurations of the Al_3O molecule, with the XY_3 symmetry, shown together with the three intermediate saddle point structures. In the center, we present the potential along the coordinates for the molecular isomerization (s direction) and the motion of the X unit out of the Y_3 plane (z direction).

are nearly degenerate and thus can be superimposed into three states that coincide with the three T configurations, in the considered time scale of the experiment. At the same time, eigenstates in triplets of higher energies are no longer nearly degenerate. Thus, in principle, the states needed in DQC are readily available, but we still need to pick those that assure the linearly independent coupling. A direct option is to use additional states related with the *out-of-plane* vibrational mode, coupled by the z-polarized light, as described below.

We obtain, using *ab initio* methods, the potential and electric dipole surfaces of a two dimensional (2D) subspace of the full (6D) configurational space of Al_3O [12]. The 2D subspace (see Fig. 2) includes as one coordinate, denoted by s, the motion along the minimum energy path for isomerization, and as the other coordinate, the out-of-plane bending mode motion of Al_3O along the z axis. The height of the isomerization barrier thus obtained, $\approx 320\ \mathrm{cm}^{-1}$, is in good agreement with other calculations [10]. Since the energy of the equilateral D_{3h}-symmetric Al_3O structure is very high, $\sim 9200\ \mathrm{cm}^{-1}$ [10], the inclusion of only the ground electronic surface should be sufficient for evaluation of the lower-energy end of the vibrational spectrum.

To calculate the relevant eigenstates and eigenenergies, we solve the 2D nuclear Schrödinger equation $H\phi(s,z) = E\phi(s,z)$, by using the discrete variable representation techniques [13]. The Hamiltonian for the angular momentum $J = 0$ in generalized coordinates $\{q_1, q_2\} = \{s, z\}$ and their conjugate momenta $\partial_q \equiv -i\hbar\partial/\partial q$ is given by [14]

$$H = \frac{1}{2}\sum_{q_1,q_2} \partial^*_{q_1} G_{q_1q_2}(s,z)\partial_{q_2} + u(s,z) + V(s,z). \quad (4)$$

Here, V is the potential energy of the ground potential surface of Fig. 2 and u is the "pseudopotential" [14]

$$u(s,z) = \frac{\hbar^2}{8}\sum_{q_1,q_2}\frac{\partial}{\partial q_1}\left\{G_{q_1q_2}\frac{\partial \ln|\mathbf{g}|}{\partial q_2}\right\} + \frac{1}{4}\frac{\partial \ln|\mathbf{g}|}{\partial q_1}G_{q_1q_2}\frac{\partial \ln|\mathbf{g}|}{\partial q_2}, \quad (5)$$

where $\mathbf{g}$ is the covariant and $\mathbf{G}$ is the contravariant metric tensor, respectively, given by

$$g_{q_1q_2} = m_a\frac{\partial \vec{x}_a}{\partial q_1}\cdot\frac{\partial \vec{x}_a}{\partial q_2}, \qquad G_{q_1q_2} = m_a^{-1}\frac{\partial q_1}{\partial \vec{x}_a}\cdot\frac{\partial q_2}{\partial \vec{x}_a}, \quad (6)$$

and $|\mathbf{g}|$ is the determinant of $\mathbf{g}$. Here, m_a is the mass of the ath atom in the molecule and $\vec{x}_a$ its Cartesian coordinate vector in the center-of-mass molecule-fixed frame; the summation convention over dummy indices is implied.

The vibrational levels for both the isomerization (s) and the out-of-plane (z) modes appear in triplets. Each triplet can be characterized by the $\{v_s, v_z\}$ numbers of nodes in each of the three wells and the particular mode (see also Fig. 3). It contains two degenerate and one separated eigenstates, where the level order alternates from triplet to triplet, with the lowest eigenstate being nondegenerate. In the lowest triplet $\{0, 0\}$, the level separation, $\Delta E \approx 2 \times 10^{-5}\ \mathrm{cm}^{-1}$, determines the tunneling time, $\tau_i = h/\Delta E \approx 1.6\ \mu\mathrm{s}$, between the three configurations of the molecule. These three eigenstates $|k\rangle$ $(i = 1, 2, 3)$ are shown in Fig. 3(a). We superimpose them to form the initial and final broken-symmetry wave packets, $|\Psi_i\rangle = \sum_k c_{i,k}|k\rangle$ $(i = 1, 2, 3)$, that are *localized* in the three Jahn-Teller wells, as displayed in Fig. 3(b). The three nondegenerate *delocalized* states in the $\{4, 0\}$, $\{6, 0\}$, and $\{4, 1\}$ triplets are chosen as the $|j\rangle$ intermediate states, shown in Fig. 3(c). Finally, the nondegenerate state in the $\{6, 1\}$ triplet, presented in Fig. 3(d), is used as the parking state $|0\rangle$.

The light pulses that couple the states must be quite different. Thus, the three nondegenerate intermediate states $\{4, 0\}$, $\{6, 0\}$, and $\{4, 1\}$ are coupled to the nearly degenerate localized states $|\Psi_i\rangle$ by pulses polarized in the x, y, and z directions, respectively, while they are coupled to the parking $|0\rangle$ state by pulses polarized in the z, z, and $y(x)$ directions, respectively. In this way we are able in DQC, despite the high symmetry of the Al_3O molecule, to tune the field amplitude to achieve the required linear independence of the Ω_1, Ω_2, and Ω_3 Rabi vectors.

The Rabi frequency amplitudes for both DQC steps are $\Omega_{j,k}(t) = \Omega^{\max}_{j,k}\{\exp[-(t+\tau)^2/\tau^2] + \exp[-(t-\tau)^2/\tau^2]\}$ and $\Omega_{k,0}(t) = \Omega^{\max}_{k,0}\{\exp[-(t+3\tau)^2/\tau^2] + \exp[-(t-3\tau)^2/\tau^2]\}$, with $\Omega^{\max}_{j,k} = \Omega^{\max}_{k,0} = 0.2\ \mathrm{cm}^{-1}$ and $\tau = 5$ ns. The dipole elements are of the order 10^{-3}–10^{-1} D. The duration of laser pulses is roughly

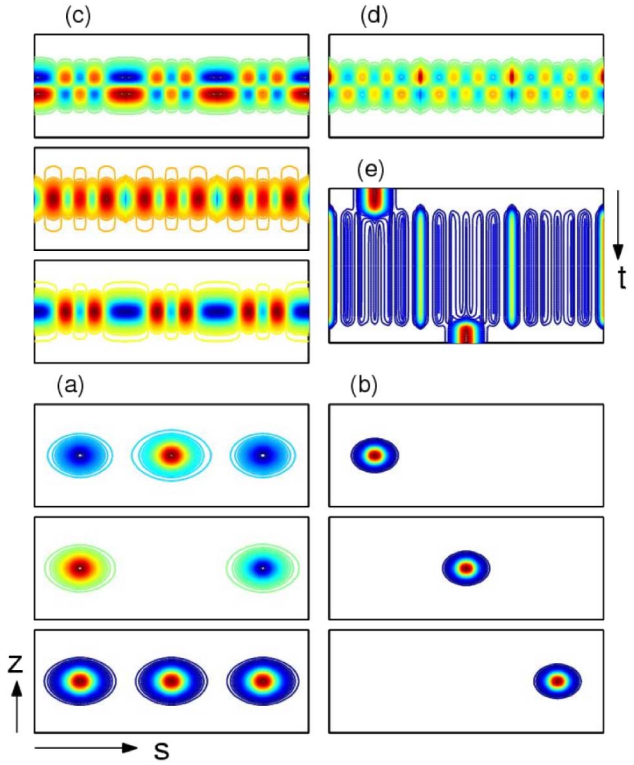

FIG. 3 (color online). (a) The three lowest energy eigenstates of the system in the s and z molecular coordinates. (b) Superpositions of these eigenstates form localized states about each Jahn-Teller well. (c),(d) The used intermediate and parking states of DQC, respectively. (e) Time-dependent DQC dynamics of the transfer between the first and second wells.

$8\tau \ll \tau_i$, so that the $|\Psi_i\rangle$ states remain localized in their corresponding potential wells for a sufficiently long time to be used as the initial states of the DQC scheme.

In Fig. 3(e), we display the time evolution of the system, during the two steps of the DQC transfer. The z-integrated probability density $\int dz|\langle s, z|\Psi(t)\rangle|^2$ is presented as a function of s and t. We start with the localized $|\Psi_1\rangle$ state being initially populated, by a selection or distillation process. At the end of step 1, its population is parked to the excited delocalized $|0\rangle$ state, using as intermediate the $|j\rangle = |1\rangle - |3\rangle$ states that remain unpopulated throughout the process. During a reasonably short parking, where we assume that a little population is lost due to relaxation, the bulk of the probability density is symmetrically concentrated near the three saddle points. Finally, at the end of the second step, the parked population is transferred to the localized $|\Psi_2\rangle$ state.

The presented control of the Jahn-Teller isomerization in the Al_3O molecule clearly demonstrates the power of the DQC solution. We can control *stable* isomers in the same way, if their intermediate states belong to an excited electronic surface. In more complex problems, we might include other physical degrees of freedom, to assure the linearly independent coupling, or even use more parking states. Besides its fundamental importance in understanding the degenerate quantum control, the presented approach could be applied in numerous practical systems, such as photoactive nanoscale devices [15].

This project was supported by the German-Israeli Foundation, the EU IHP programme HPRN-CT-1999-00129, the Office of Naval Research, USA, and the Swiss Friends of the Weizmann Institute.

[1] M. Shapiro and P. Brumer, *Principles of the Quantum Control of Molecular Processes* (Wiley, New York, 2003).
[2] D. G. Grischkowski, M. M. T. Loy, and P. F. Liao, Phys. Rev. A **12**, 2514 (1975); J. Oreg, F. T. Hioe, and J. H. Eberly, Phys. Rev. A **29**, 690 (1984).
[3] U. Gaubatz, P. Rudecki, S. Schiemann, and K. Bergmann, J. Chem. Phys. **92**, 5363 (1990); K. Bergmann, H. Theuer, and B. W. Shore, Rev. Mod. Phys. **70**, 1003 (1998).
[4] P. Král and M. Shapiro, Phys. Rev. Lett. **87**, 183002 (2001); P. Král, I. Thanopulos, M. Shapiro, and D. Cohen, Phys. Rev. Lett. **90**, 033001 (2003); I. Thanopulos, P. Král, and M. Shapiro, J. Chem. Phys. **119**, 5105 (2003).
[5] P. Marte, P. Zoller, and J. L. Hall, Phys. Rev. A **44**, R4118 (1991).
[6] R. Unanyan, M. Fleischhauer, B. W. Shore, and K. Bergmann, Opt. Commun. **155**, 144 (1998); H. Theur *et al.*, Opt. Express **4**, 77 (1999); R. G. Unanyan, B. W. Shore, and K. Bergmann, Phys. Rev. A **63**, 043401 (2001).
[7] Z. Kis and S. Stenholm, Phys. Rev. A **64**, 063406 (2001); Z. Kis and F. Renzoni, *ibid.* **65**, 32318 (2002); A. Karpati and Z. Kis, J. Phys. B **36**, 905 (2003).
[8] P. Král, Z. Amitay, and M. Shapiro, Phys. Rev. Lett. **89**, 063002 (2002).
[9] P. R. Bunker and P. Jensen, *Molecular Symmetry and Spectroscopy* (NRC Research Press, Ottawa, 1998), 2nd ed.
[10] A. I. Boldyrev and P. von R. Schleyer, J. Am. Chem. Soc. **113**, 9045 (1991); T. K. Ghanty and E. R. Davidson, J. Phys. Chem. A **103**, 2867 (1999).
[11] S. Stevenson *et al.*, Nature (London) **401**, 55 (1999); L. Alvarez *et al.*, Phys. Rev. B **66**, 035107 (2002).
[12] The 2D potential energy and electric dipole surfaces are obtained at the PUMP2 level of theory using the 6-31G* basis set. However, the minimum and saddle point molecular structures are optimized at the PUMP2 (full) level of theory with the same basis set.
[13] J. C. Light and T. Carrington, Jr., Adv. Chem. Phys. **114**, 263 (2000); S. Kanfer and M. Shapiro, J. Phys. Chem. **88**, 3964 (1984).
[14] D. Luckhaus, J. Chem. Phys. **113**, 1329 (2000).
[15] V. Balzani, A. Credi, F. M. Raymo, and J. F. Stoddart, Angew. Chem., Int. Ed. Engl. **39**, 3348 (2000).